ADVANCES IN ATMOSPHERIC SCIENCES, VOL. 38, JULY 2021, 1165–1176

• **Original Paper** •

Vertical Evolution of Boundary Layer Volatile Organic Compounds in Summer over the North China Plain and the Differences with Winter

Shuang WU[1,4], Guiqian TANG[*1,2,4], Yinghong WANG[1], Rong MAI[3], Dan YAO[1,2,4], Yanyu KANG[1,5], Qinglu WANG[1,4], and Yuesi WANG[1,2,4]

[1]*State Key Laboratory of Atmospheric Boundary Layer Physics and Atmospheric Chemistry, Institute of Atmospheric Physics, Chinese Academy of Sciences, Beijing* 100029, *China*

[2]*Center for Excellence in Regional Atmospheric Environment, Institute of Urban Environment, Chinese Academy of Sciences, Xiamen* 361021, *China*

[3]*Weather Modification Office of Hebei Province, Shijiazhuang* 050021, *China*

[4]*University of Chinese Academy of Sciences, Beijing* 100049, *China*

[5]*Anhui University, Hefei* 230601, *China*

(Received 6 August 2020; revised 2 November 2020; accepted 6 November 2020)

ABSTRACT

The vertical observation of volatile organic compounds (VOCs) is an important means to clarify the mechanisms of ozone formation. To explore the vertical evolution of VOCs in summer, a field campaign using a tethered balloon during summer photochemical pollution was conducted in Shijiazhuang from 8 June to 3 July 2019. A total of 192 samples were collected, 23 vertical profiles were obtained, and the concentrations of 87 VOCs were measured. The range of the total VOC concentration was 41–48 ppbv below 600 m. It then slightly increased above 600 m, and rose to 58 ± 52 ppbv at 1000 m. The proportion of alkanes increased with height, while the proportions of alkenes, halohydrocarbons and acetylene decreased. The proportion of aromatics remained almost unchanged. A comparison with the results of a winter field campaign during 8–16 January 2019 showed that the concentrations of all VOCs in winter except for halohydrocarbons were more than twice those in summer. Alkanes accounted for the same proportion in winter and summer. Alkenes, aromatics, and acetylene accounted for higher proportions in winter, while halohydrocarbons accounted for a higher proportion in summer. There were five VOC sources in the vertical direction. The proportions of gasoline vehicular emissions + industrial sources and coal burning were higher in winter. The proportions of biogenic sources + long-range transport, solvent usage, and diesel vehicular emissions were higher in summer. From the surface to 1000 m, the proportion of gasoline vehicular emissions + industrial sources gradually increased.

Key words: volatile organic compounds, vertical profile, planetary boundary layer, source apportionment

Citation: Wu, S., G. Q. Tang, Y. H. Wang, R. Mai, D. Yao, Y. Y. Kang, Q. L. Wang, and Y. S. Wang, 2021: Vertical evolution of boundary layer volatile organic compounds in summer over the North China Plain and the differences with winter. *Adv. Atmos. Sci.*, **38**(7), 1165−1176, https://doi.org/10.1007/s00376-020-0254-9.

Article Highlights:

- The VOC concentration slightly increased with height in the boundary layer in summer.
- The VOC concentration in summer was significantly lower than that in winter.
- The source contribution of gasoline vehicular emissions + industrial sources increased with height.

1. Introduction

Volatile organic compounds (VOCs) are important atmospheric pollutants that can react with nitrogen oxides (NO_x) as precursors under ultraviolet radiation to generate secondary pollutants such as ozone (O_3). O_3 is the main component of photochemical smog and one of the main indicators to measure its intensity (Tang et al., 2009; Seinfeld and Pandis, 2016). O_3 has a nonnegligible effect on global warming as an important greenhouse gas (Akimoto, 2003). In addition, near-ground O_3 can irritate human eyes and respiratory systems, cause air quality deterioration, and harm plant growth (Yue et al., 2017). Since the implementation of the "Action Plan for Prevention and Control of Air Pollution", the concentrations of $PM_{2.5}$, sulfur dioxide (SO_2), and NO_x

* Corresponding author: Guiqian TANG
Email: tgq@dq.cern.ac.cn

in most areas of China have decreased compared with those in previous years, but the O_3 concentrations in many areas, including the North China Plain, have increased year by year (Zhang et al., 2014, 2019; Ma et al., 2016; Gao et al., 2017; Tang et al., 2021). Photochemical pollution is a serious problem, but the mechanisms are not fully understood.

Studies have shown that most O_3 is not generated near the ground and that vertical transport from the upper boundary layer is the main source of O_3 near the ground (Tang et al., 2017; Chen et al., 2018; Yang et al., 2020). Nitrogen dioxide is transported by convection at noon to the upper boundary layer, where photolysis is performed to form O_3. Simultaneously, the O_3 formed in the upper boundary layer will be quickly transported to near the ground to react with nitric oxide and compensate for the loss caused by the reaction (Tang et al., 2017, 2021). This vertical exchange mechanism has led to a higher O_3 concentration in the upper boundary layer (Zheng et al., 2005; Chen et al., 2013; Ma et al., 2013; Zhao et al., 2019). Therefore, not only should O_3 prevention strategies be based on near-ground observation data, but the generation sensitivity of O_3 in the upper atmosphere should be considered. Numerical simulation results have shown that the concentration of NO_x in the boundary layer decreases more rapidly than that of VOCs, and this phenomenon causes VOCs/NO_x to gradually increase with height. O_3 generation is sensitive to VOCs near the ground and tends to be sensitive to NO_x as the height increases (Spirig et al., 2002; Chen et al., 2013). However, the above results lack the verification of observation data to recognize the vertical evolution of the precursors of O_3. Therefore, there is an urgent need to carry out vertical observation research to clarify the evolution mechanisms of O_3 and its precursors in the atmosphere.

According to previous studies, the concentration of VOCs decreases with height (Bonsang et al., 1991; Wöhrnschimmel et al., 2006; Mao et al., 2008; Schnitzhofer et al., 2009; Sun et al., 2018; Zhang et al., 2018). By vertical mixing and photochemical loss in the mixing layer (ML), the concentration can decrease by 74%–95% (Sangiorgi et al., 2011). A vertical exponential pattern was also observed (Koßmann et al., 1996). The results of Wu et al. (2020) in Shijiazhuang in January 2019 showed that the VOC concentration decreased below 1000 m, decreasing faster from the surface to 400 m than that from 400 m to 1000 m. Alkanes accounted for the largest proportion, which increased from 60.2% to 79.0% with height. The proportions of alkenes, halohydrocarbons, and acetylene decreased with height. The proportion of aromatics remained at approximately 11%. At night, the VOC concentration and secondary organic aerosol formation potential were lower in the residual layer (RL).

In this study, Shijiazhuang, the city with the most serious photochemical pollution on the North China Plain (Tang et al., 2012), was taken as an example. The concentration of VOCs below 1000 m was observed vertically using miniaturized instruments carried by a tethered balloon. Tethered balloon observation has certain advantages over other observational methods, such as tower, aircraft, or unmanned aerial vehicle observation. Tethered balloon observation can explore the vertical evolution of VOCs in the planetary boundary layer (PBL) effectively (Sun et al., 2018; Zhang et al., 2018; Wu et al., 2020). In this study, the vertical evolution characteristics of VOC concentration and reactivity in the PBL above Shijiazhuang in summer are described, the differences in winter and summer compared, and vertical source apportionment in the PBL performed.

2. Data and methods

2.1. *Experimental site and period*

To avoid heavy precipitation in July and August, the experimental period was scheduled from 8 June to 3 July 2019. The Yuanshi National Meteorological Observing Station (37°48′N, 114°30′E) in Yuanshi County, Shijiazhuang, was selected to conduct the field campaign. A description of this site has been provided in Wu et al. (2020). Two observational experiments were conducted each day on fair days with low wind speeds, before sunrise (0400 LST to 0500 LST) and in the afternoon (1400 LST to 1600 LST).

2.2. *Data*

2.2.1. *VOC concentrations*

The experimental system and methods for collecting VOC samples in this study were the same as employed in Wu et al. (2020). Ultimately, a total of 192 samples were collected, and 23 vertical profiles (14 before sunrise and 9 in the afternoon) were obtained in the field campaign. Measurement of all samples was conducted in a laboratory in Beijing. Preconcentration was conducted with a TH-300B system (Wuhan Tianhong Environmental Protection Industry Co., Ltd., China); C_2–C_5 hydrocarbons were measured with a flame ionization detector; and C_6–C_{11} hydrocarbons, aromatics and halohydrocarbons were measured by mass spectrometry. All measured compounds (87 in total) and their method detection limits (MDLs) are listed in Table S1 [in the electronic supplementary material (ESM)].

2.2.2. *Other data*

Vertical meteorological variables were measured using a meteorological sensor (XLS-II, Institute of Atmospheric Physics, Chinese Academy of Sciences, China) (Sun et al., 2018; Zhao et al., 2019; Wu et al., 2020). The determination of the heights of different layers in the PBL paralleled that of Wu et al. (2020). Measurement was also assisted by the observations of a ceilometer (CL51, Vaisala, Finland) (Tang et al., 2015).

2.3. *Data analysis methods*

2.3.1. *SAPRC mechanisms*

The Statewide Air Pollution Research Center (SAPRC) mechanisms are widely used in current models. Different organic molecules are classified according to their reactivities with hydroxy groups (OH) (Carter, 2010; Carter and

Heo, 2013). Alkanes, alkenes, and aromatics are classified into 12 categories in total (including 5, 4 and 3 categories, respectively). The compounds within each category are shown in Table S2.

2.3.2. *Calculation of the OH and NO_3 loss rates*

The loss rates of OH and nitrate (NO_3) radicals were calculated and used to analyze the reactivities of VOCs during the day and night. The OH loss rate (L_{OH}) and NO_3 loss rate (L_{NO_3}) of VOC_i are calculated as follows:

$$L_{OH} = \sum [VOC]_i \times K_{i,OH} , \quad (1a)$$

$$K_{i,OH} = A_{1i} T^{n_{1i}} e^{-B_{1i}T} , \quad (1b)$$

$$L_{NO_3} = \sum [VOC]_i \times K_{i,NO_3} , \quad (2a)$$

$$K_{i,NO_3} = A_{2i} T^{n_{2i}} e^{-B_{2i}T} , \quad (2b)$$

where $[VOC]_i$ denotes the concentration of VOC_i. A_{1i}, B_{1i}, n_{1i}, A_{2i}, B_{2i} and n_{2i} are the corresponding parameters of species VOC_i. $K_{i,OH}$ and K_{i,NO_3} are reaction rate constants that change with temperature (Atkinson and Arey, 2003).

2.3.3. *Positive matrix factorization*

A positive matrix factorization (PMF) model is an advanced multivariate factor analysis method that has been widely used to identify the main sources of atmospheric pollutants and quantify their contributions (Paatero and Tapper, 1994; Paatero, 1997). In this study, PMF 5.0 was used to analyze the sources of VOCs during the observation period. To run the PMF model, concentration and uncertainty data need to be input. If a concentration is below its MDL, it should be determined by MDL/2 instead (Richard et al., 2011). The uncertainty data can be calculated based on the MDL and error fraction (the error fraction of species *i* was calculated as $EF_i = \sigma_i / C_i$, where C_i is the average concentration of the gas standard that was repeatedly measured seven times and σ_i is the standard deviation of concentration) as follows: if a concentration value is less than or equal to its MDL, the uncertainty will be 5/6 MDL; for a concentration value higher than its MDL, the uncertainty should be calculated by the following equation (PMF 5.0 User Guide):

$$U_{nc} = \sqrt{(EF \times C)^2 + (0.5 \times MDL)^2} . \quad (3)$$

3. Results and discussion

3.1. *Vertical evolution of the VOC concentration*

A total of 23 vertical profiles were obtained below 1000 m, and the average concentrations and proportions were calculated (Fig. 1). The range of the total volatile

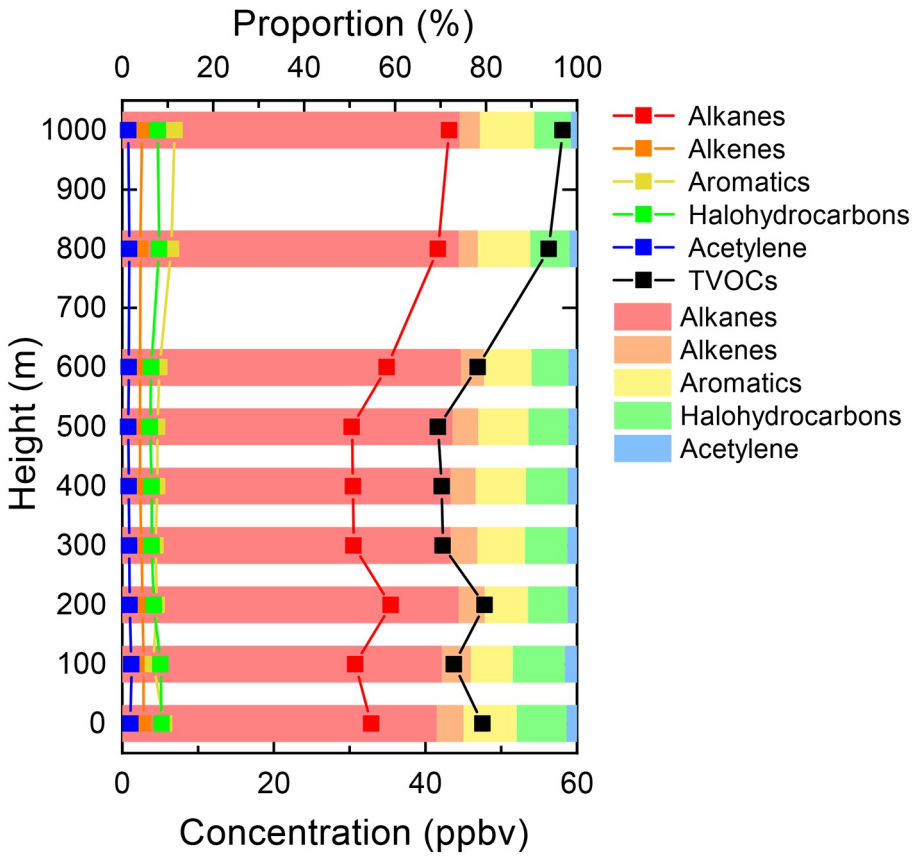

Fig. 1. Vertical profiles and proportions of the average concentrations of VOCs.

organic compound (TVOC) concentration was 41–48 ppbv below 600 m. It then slightly increased above 600 m, and rose to 58 ± 52 ppbv at 1000 m. From the surface to 1000 m, the average rate of increase was 1.1 ppbv hm^{-1}, with a rate of increase of 2.8 ppbv hm^{-1} from 600 m to 1000 m. Similar to that of the TVOC concentration, the range of the alkane concentration was 30–35 ppbv below 600 m. It then slightly increased above 600 m and rose to 43 ± 44 ppbv at 1000 m. Changing very little at different heights, the concentration ranges of alkenes, aromatics and halohydrocarbons were 2–3 ppbv, 4–7 ppbv and 3–6 ppbv, respectively. The concentration of acetylene was approximately 1 ppbv at each height. Alkanes accounted for the largest proportion at each height; their proportion gradually increased from the surface (69.1%) to 600 m (74.5%) and remained almost unchanged from 600 m to 1000 m. Alkenes, halohydrocarbons and acetylene accounted for the highest proportions at 100 m, 6.4%, 11.4% and 2.7%, respectively, and gradually decreased to 4.4%, 8.1% and 1.4%, respectively, at 1000 m. The proportion of aromatics changed very little (approximately 11%). The concentration of isopentane was the highest among those of all compounds at each height. The average concentrations of measured VOCs at different heights are shown in Table S3 in the ESM. The average concentrations of some alkenes such as 1,3-butadiene and trans-2-pentene, some aromatics such as p-ethyltoluene and m-ethyltoluene, and some halohydrocarbons such as bromoform and 1,2-dibromoethane, were below their MDLs at different heights.

3.2. *Vertical evolution of the VOC reactivity*

According to the SAPRC mechanisms, the vertical profiles and proportions of the average concentrations (Fig. 2a), L_{OH} (Fig. 2b), and L_{NO_3} (Fig. 2c) of the 12 categories of VOCs were obtained (Wu et al., 2020). The concentration of ALK4 was the highest at each height, with a range of 21–27 ppbv below 600 m. This concentration then slightly increased above 600 m, and rose to 35 ppbv at 1000 m. The proportion increased from 56.9% to 66.6% with height. The concentrations of other VOCs were below 4 ppbv at each height. The L_{OH} of ALK4 and ARO2 was approximately 2 s^{-1} below 600 m and slightly increased above that, rising to 2.8 s^{-1} and 3.6 s^{-1} at 1000 m, respectively. ALK4 accounted for a proportion of approximately 30% at each height, and the proportion of ARO2 increased from 27.1% to 39.5% with height. The proportion of L_{OH} of OLE2 decreased from 17.1% to 10.5% with height. Since NO_3 radicals play an important role at night, the samples collected before sunrise were chosen to analyze L_{NO_3}. ARO2 accounted for 89.2% of L_{NO_3} at the surface, increasing to 96.5% at 1000 m, of which styrene accounted for more than 99.9%. Isoprene accounted for 7.8% at the surface, decreasing to 2.5% at 1000 m. Other VOCs accounted for less than 3% of L_{NO_3} at each height.

3.3. *Vertical evolution of the ratios of typical species*

The ratios of some typical VOCs were also calculated (Fig. 3). The ratio of the average concentrations of toluene to benzene (*T*/*B*) gradually increased with height (ranging from 4.1 to 7.9). When T/B is > 2, according to previous studies (Han et al., 2020), VOCs are affected by industrial sources in addition to vehicle exhaust emissions. The increasing trend of this ratio indicated the important role of industrial sources at high altitudes. The ratio of the average concentrations of m/p-xylene to ethylbenzene (*X*/*E*) gradually decreased with height (ranging from 0.38 to 0.62). This ratio is often used as an indicator of the degree of air mass aging because m/p-xylene has a higher reaction rate with OH radicals (Sun et al., 2018; Han et al., 2020). The decreasing trend of this ratio indicated a higher degree of air mass aging at high altitudes. Moreover, when *X*/*E* is substantially < 3 (Yurdakul et al., 2018), VOCs are affected by long-range transport. Source apportionment results are presented in section 3.4.2.

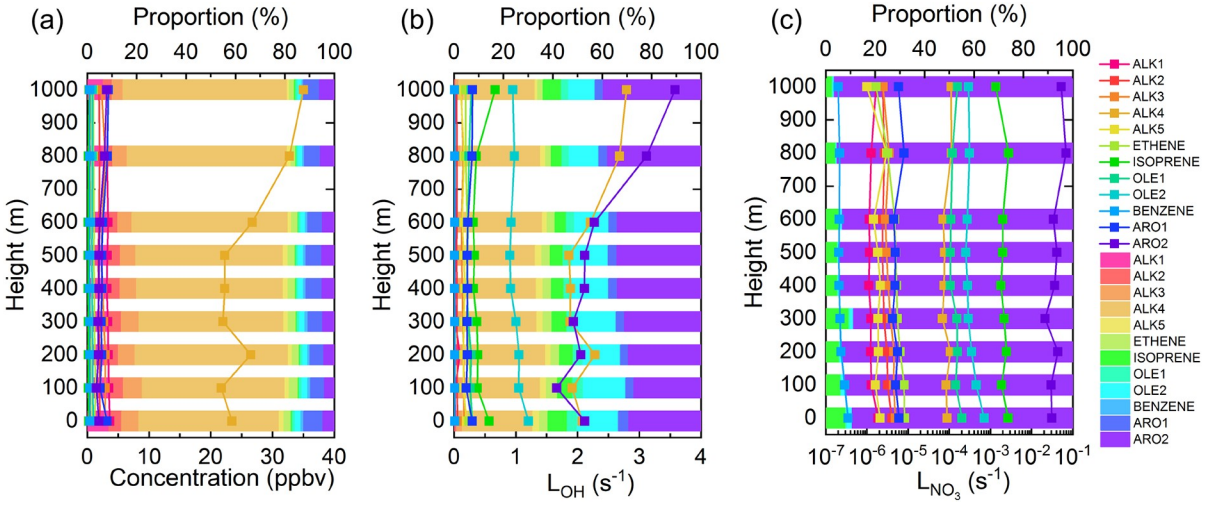

Fig. 2. Vertical profiles and proportions of the average (a) concentration, (b) L_{OH}, and (c) L_{NO_3} of alkanes, alkenes, and aromatics with different reactivities.

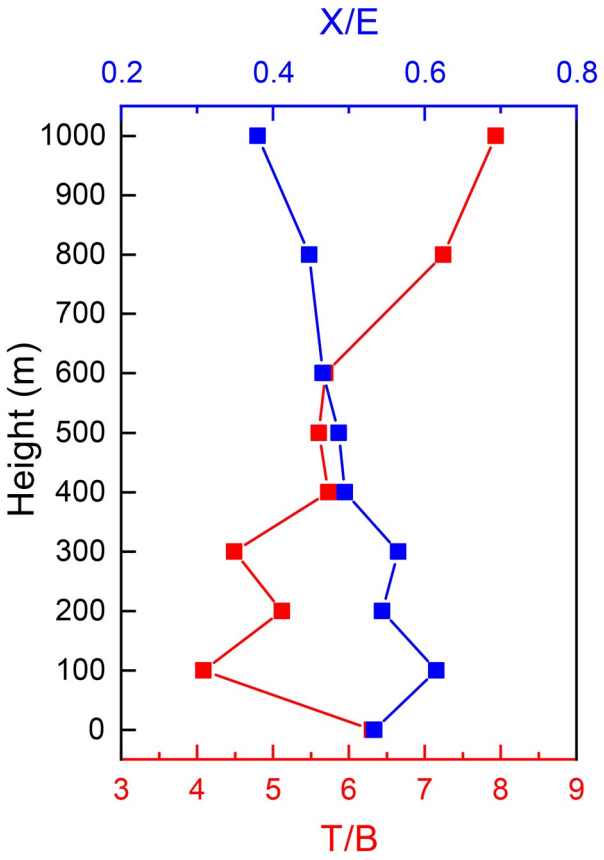

Fig. 3. Vertical evolution of the ratios of the average concentrations of toluene to benzene (*T*/*B*) and m/p-xylene to ethylbenzene (*X*/*E*).

3.4. *Comparison of VOC vertical evolution characteristics and source apportionment in winter and summer*

The winter field campaign for VOC vertical observation was carried out in Yuanshi County, Shijiazhuang, in January 2019 (Wu et al., 2020). In this section, the vertical evolution characteristics of VOCs in winter and summer are compared, and their vertical source apportionment presented.

3.4.1. *Comparison of the vertical evolution of VOC concentrations and proportions in winter and summer*

The vertical evolution characteristics of VOC concentrations in winter and summer exhibited significant differences. Except for that of halohydrocarbons, the concentrations of other VOCs in winter were more than twice those in summer (Fig. 4), and the ratios between the concentrations in winter and summer were the highest at the surface, decreasing with height. The ratios of alkanes and aromatics were 4.4 and 5.7 at 100 m, respectively, and decreased to 2.4 and 2.3 at 1000 m. The difference in the concentration of alkanes between winter and summer was 105.5 ppbv at 200 m and 60.9 ppbv at 1000 m. The difference in the concentration of aromatics was 20.5 ppbv at the surface and 8.8 ppbv at 1000 m. The ratios of alkenes and acetylene were 9.5 and 8.7 at the surface, respectively, and decreased to 2.3 and 3.0 at 1000 m. The difference in the concentration of alkenes between winter and summer was 24.2 ppbv at the surface and 3.4 ppbv at 1000 m. The difference in the concentration of acetylene was 8.5 ppbv at the surface and 1.6 ppbv at 1000 m. The ratio of halohydrocarbons at the surface was 5.4, with a concentration difference of 22.9 ppbv. This ratio decreased to 0.9 and 0.8 at 800 m and 1000 m, respectively, indicating that the concentration in summer was higher than that in winter. The ratio of TVOCs decreased from 4.8 at the surface to 2.3 at 1000 m, and the concentration difference decreased from 180.7 ppbv to 73.6 ppbv.

The average proportions of VOCs in winter and summer also differed (Fig. 5). The proportions of alkenes, aromatics and acetylene were 7% ± 2%, 12% ± 1% and 3% ± 1%, respectively, in winter, which were higher than the proportions of 5% ± 1%, 11% ± 1% and 2% ± 0.4%, respectively, in summer. The proportion of halohydrocarbons in summer was 9% ± 1%, which was higher than the proportion of 5% ± 3% in winter. The proportion of alkanes was the same in winter (73% ± 6%) and summer (73% ± 2%).

To explore the differences in the concentrations of VOCs in the stable boundary layer (SBL) and RL at night, and in the ML during the day, in summer, 14 vertical profiles observed before sunrise and 9 profiles observed in the afternoon were used to calculate the VOC concentrations in the three layers (Table 1). The sample sizes were 45, 59 and 76, respectively. The concentrations and proportions of VOCs in the SBL and RL at night exhibited little difference, and alkanes accounted for more than 70%. The TVOC concentration in the ML in the daytime was 50 ± 41 ppbv, which was approximately 5 ppbv higher than those in the SBL and RL at night, while the proportions of VOCs exhibited little difference. The relatively uniform pattern in different layers may be caused by strong convection and high PBL heights in summer. Compared with those in winter (Wu et al., 2020), the concentrations of VOCs in the three layers in summer decreased significantly, constituting 19%, 25% and 32% in the SBL and RL at night and the ML in the daytime, respectively, of those in winter.

3.4.2. *Vertical source apportionment of VOCs*

A large number of previous studies have focused on VOC sources near the ground, lacking an understanding of the sources in the vertical direction. However, it is conducive to the understanding and regulation of VOCs to explore the sources in the vertical direction and clarify the differences in different layers of the PBL. Based on the 275 samples collected in the field campaigns (83 in winter and 192 in summer), 34 VOCs were selected as sample species for the PMF operation (Fig. S1 in the ESM), accounting for 94% of the TVOC concentration. The sample species included 12 alkanes, 5 alkenes, 10 aromatics, 5 halohydrocarbons, and acetylene. In addition, acetone was also selected as a tracer of solvent usage (some oxygenated volatile organic compounds were also measured in the experiments). The chosen species had relatively high concentrations and they are typical tracers for specific sources.

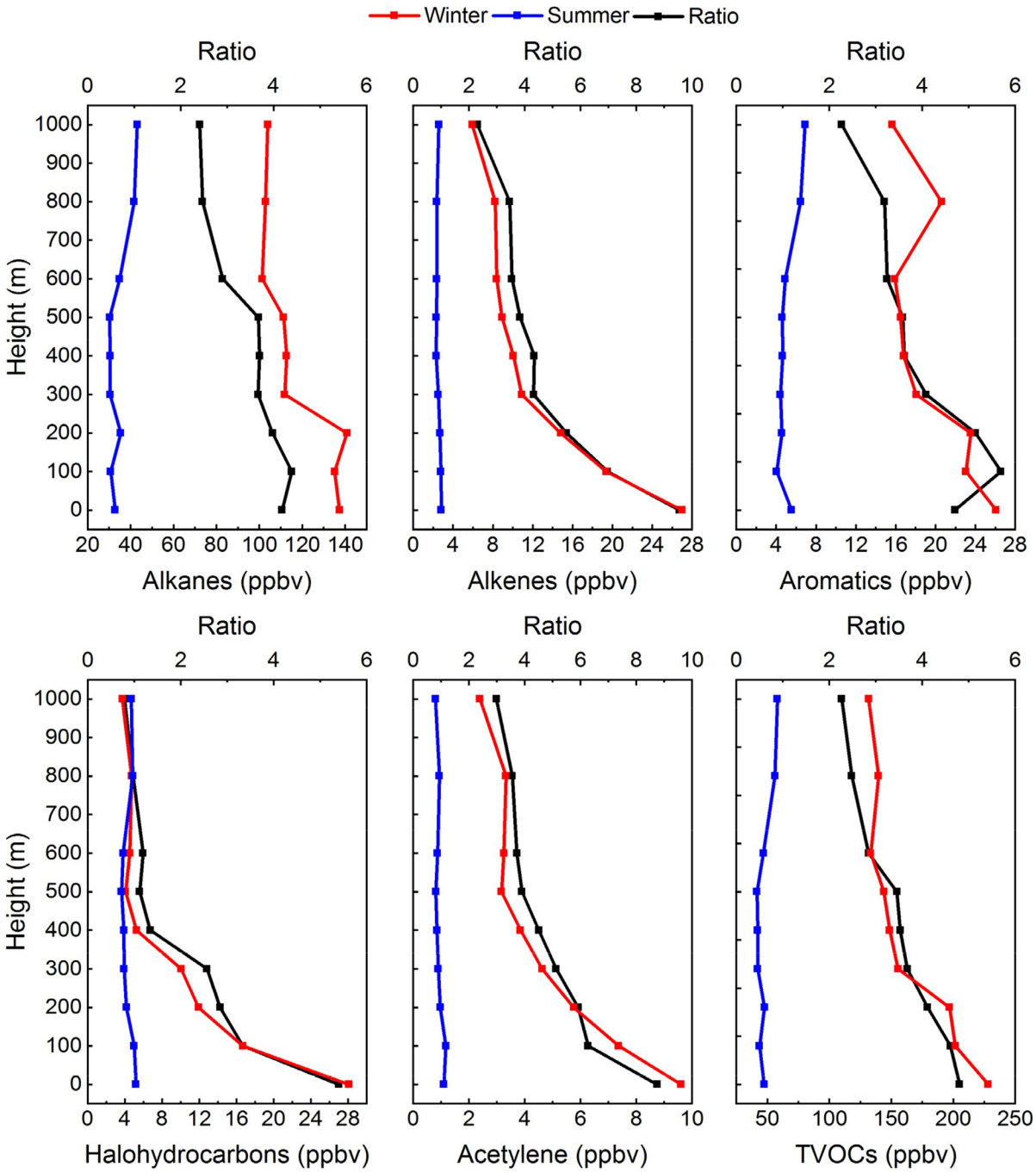

Fig. 4. Comparison of the average concentrations of VOCs in winter and summer.

Finally, through the identification of chemical tracers, five pollution sources were identified, including gasoline vehicular emissions + industrial sources, diesel vehicular emissions, coal burning, solvent usage, and biogenic sources + long-range transport.

Factor 1 was gasoline vehicular emissions + industrial sources. N-pentane (87.2%), isopentane (86.3%), isobutane (81.5%), and n-butane (40.9%) are tracers of gasoline vehicular emissions (Cai et al., 2010; Sun et al., 2016; Liu et al., 2017). Styrene (84.3%), 1-pentene (82.7%), toluene (66.3%), and ethylbenzene (43.5%) are tracers of industrial sources (Chen et al., 2014; Liu et al., 2017; Yang et al., 2019). Factor 2 was diesel vehicular emissions. Among them, undecane (77.3%), n-nonane (72.5%), n-octane (39.0%), and n-decane (33.0%) are important tracers for this factor (Liu et al., 2008; Sun et al., 2016). The proportions of m-diethylbenzene (32.7%), 1,2,3-trimethylbenzene (27.9%), 1,2,4-trimethylbenzene (14.8%), and 1,3,5-trimethylbenzene (12.3%) also indicated that factor 2 was related to combustion (Liu et al., 2008). Factor 3 was coal burning. Ethene (80.1%), propene (73.3%), acetylene (70.1%), benzene (67.4%), 1,2-dichloroethane (66.0%), chloromethane

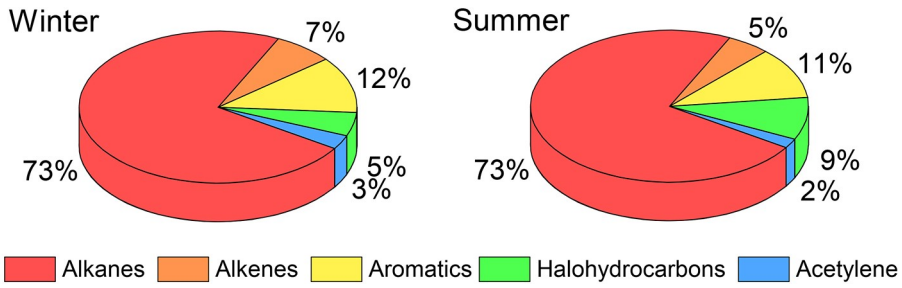

Fig. 5. Comparison of the proportions of the average VOC concentrations in winter and summer at different heights.

Table 1. Average VOC concentrations in the SBL and RL at night and the ML during the day in summer.

Concentration (ppbv)	SBL (n = 45)	RL (n = 59)	ML (n = 76)
Alkanes	32 ± 38	34 ± 37	36 ± 35
Alkenes	3 ± 1	2 ± 1	3 ± 1
Aromatics	4 ± 5	5 ± 6	5 ± 5
Halohydrocarbons	4 ± 3	3 ± 1	5 ± 3
Acetylene	1 ± 1	1 ± 0	1 ± 1
TVOCs	44 ± 44	45 ± 44	50 ± 41

(54.5%), and 1-butene (47.9%) are typical species emitted into the atmosphere during coal burning (Cai et al., 2010; Islam et al., 2020). Factor 4 was solvent usage. O-xylene (56.9%), acetone (48.4%), m/p-xylene (42.5%), and ethylbenzene (35.4%) are common main components in coatings and paints and are used as additives and adhesives in many industrial processes, such as in the textile industry (Chen et al., 2014; Liu et al., 2017). Factor 5 was biogenic sources + long-range transport. Isoprene (62.4%) is an important VOC emitted by plants. Freon-11 (50.8%), freon-113 (48.6%), and carbon tetrachloride (42.2%) are tracers transported over long distances (Yang et al., 2019; Liu et al., 2020).

Based on the PMF operation results, the proportions of the five sources were calculated (Fig. S2 in the ESM). Gasoline vehicular emissions + industrial sources (60.1%) were the main sources of pollution, followed by coal burning (15.8%), biogenic sources + long-range transport (14.7%), solvent usage (7.9%), and diesel vehicular emissions (1.5%). Therefore, efforts should be made to address these pollution sources for emissions reduction and regulation of VOCs in Shijiazhuang. Measures should be taken to limit the exhaust emissions of motor vehicles to reduce VOC pollution considering the high concentration and proportion of alkanes. Emission standards should be raised and oil quality should be improved to control vehicular emissions. Currently, China has strict emission standards but undeveloped oil quality, so it is more urgent to improve oil quality (Tang et al., 2016).

The PMF operation results were classified according to seasons, and the contributions of VOC pollution sources in winter and summer were extracted (Fig. 6). Gasoline vehicular emissions + industrial sources accounted for the largest proportion in both seasons and were higher in winter (69.7%) than in summer (50.2%). The proportion of coal burning in winter (21.9%) was significantly higher than that in summer (6.2%), demonstrating the considerable contribution of heating in winter. The proportion of biogenic sources + long-range transport was significantly higher in summer (28.0%) than in winter (4.0%). This may be caused by lush vegetation in summer, and the average PBL height in summer (996 ± 704 m) was three times that in winter (332 ± 279 m). A lower PBL height and a larger proportion of coal burning in winter indicated that local sources were the main contributors. The proportion of solvent usage in summer (12.2%) was higher than that in winter (4.2%), and this result may be caused by the high temperature and increased evaporation of solvents in summer. Diesel vehicular emissions were the lowest emission source and were higher in summer (3.4%) than in winter (0.2%).

The PMF operation results were categorized according to different heights and layers. The vertical evolution of pollution source contributions was explored (Fig. 7), and the contributions of VOC pollution sources in different layers of the PBL in both winter and summer were extracted (Fig. 8). The sample sizes in the SBL, RL and ML in the winter were 25, 32 and 26, respectively; the sample sizes in the SBL, RL and ML in the summer were 45, 63 and 84, respectively.

In winter, the proportions of gasoline vehicular emissions + industrial sources and solvent usage gradually increased from the surface to 1000 m (Fig. 7a), from 55.7% and 2.7% at the surface to 80.8% and 6.9% at 1000 m, respectively. In contrast, the proportion of coal burning decreased from 37.9% to 8.9%. The proportions of diesel vehicular emissions and biogenic sources + long-range transport exhibited little difference. In each layer of the PBL (Fig. 8a), gasoline vehicular emissions + industrial sources and coal burning were the main pollution sources. Gasoline vehicular emissions + industrial sources accounted for the highest proportion in the RL (80.4%) and the lowest in the ML (52.1%). Diesel vehicular emissions accounted for a slightly higher proportion in the ML (0.3%). Coal burning and biogenic sources + long-range transport accounted for the highest proportions in the ML (36.8% and 6.9%, respectively) and the lowest in the RL (11.0% and 2.8%, respectively). Solvent usage accounted for the highest proportion in the RL (5.7%) and the lowest in the SBL (2.9%).

The proportion of gasoline vehicular emissions + indus-

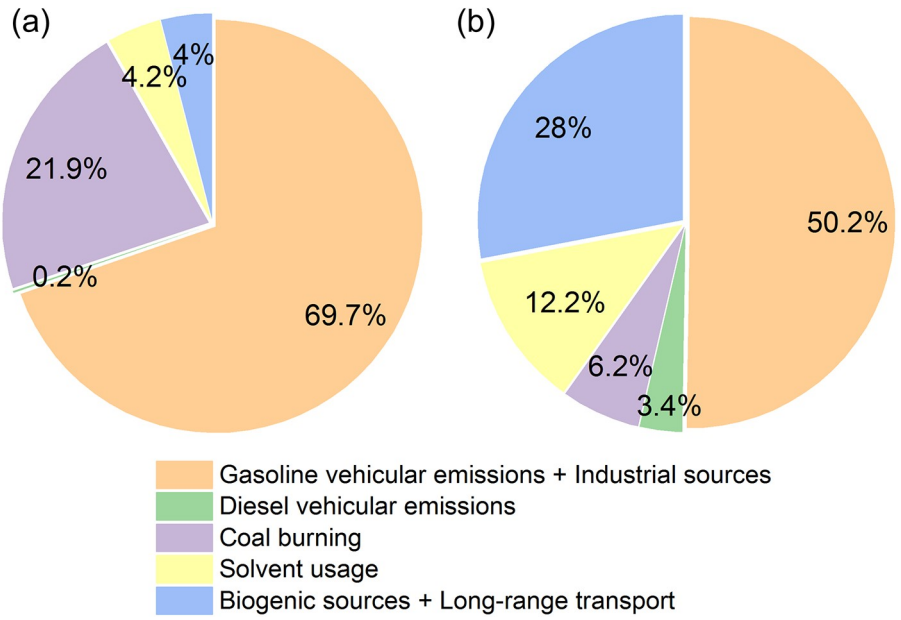

Fig. 6. Vertical source contributions of VOCs in Shijiazhuang in (a) winter and (b) summer derived by PMF.

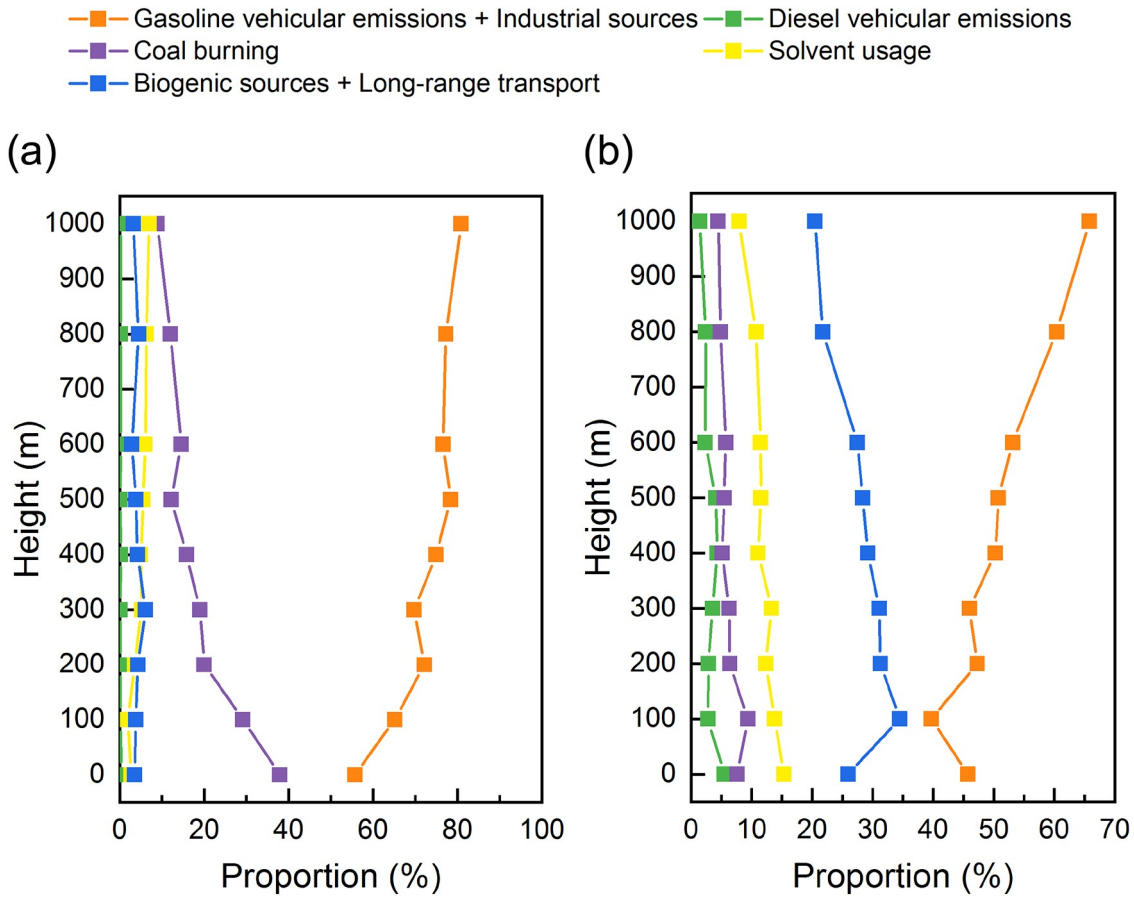

Fig. 7. Vertical evolution of the VOC source contributions in the PBL above Shijiazhuang in (a) winter and (b) summer derived by PMF.

trial sources gradually increased in summer (Fig. 7b), with the lowest value at 100 m (39.7%) and the highest at 1000 m (65.8%). The proportions of the other four sources gradually decreased. Biogenic sources + long-range transport and coal burning accounted for proportions of 34.5% and 9.4% at 100 m and these proportions fell to 20.4% and 4.5% at

1000 m. Solvent usage and diesel vehicular emissions accounted for proportions of 15.3% and 5.5% at the surface, and these proportions decreased to 7.9% and 1.4% at 1000 m, respectively. In each layer of the PBL (Fig. 8b), gasoline vehicular emissions + industrial sources, biogenic sources + long-range transport, and solvent usage were the main pollution sources. The proportion of gasoline vehicular emission + industrial sources was highest in the ML (52.6%) and lowest in the SBL (42.2%). The proportions of biogenic sources + long-range transport and coal burning were the highest in the SBL (30.9% and 9.6%, respectively) and the lowest in the RL (26.2% and 4.0%, respectively). Solvent usage and diesel vehicular emissions accounted for the highest proportions in the RL (14.2% and 3.8%, respectively) and the lowest in the ML (10.2% and 3.0%, respectively).

Due to the long lifetime and low reactivity of VOCs such as isopentane emitted by gasoline vehicles, the concentration decreased slowly with height. Therefore, the proportion of gasoline vehicular emissions + industrial sources in winter and summer gradually increased with height and was higher in the RL than in the SBL. Since gasoline vehicular emissions were concentrated near the ground, indicating the important role of industrial sources at high altitudes, industry may be the main source of high-altitude VOC reactivity. High-carbon alkanes also have a long lifetime in the atmosphere, so the proportion of diesel vehicular emissions in the RL was higher than that in the SBL in summer. Coal burning usually emits alkenes and aromatics with high reactivities, which decrease rapidly with height, so the proportion of coal burning decreased with height, and the proportion in the SBL was higher than that in the RL. Since the VOCs emitted by vegetation come from near the ground, the proportion of biogenic sources + long-range transport decreased with height and the proportion in the SBL was higher than that in the RL.

4. Conclusions

The vertical observation of VOCs is an important means to clarify the formation mechanisms of O_3. To explore the vertical evolution characteristics of VOCs, a field campaign using a tethered balloon during summer photochemical pollution was conducted in Shijiazhuang from 8 June to 3 July 2019. The TVOC concentration was relat-

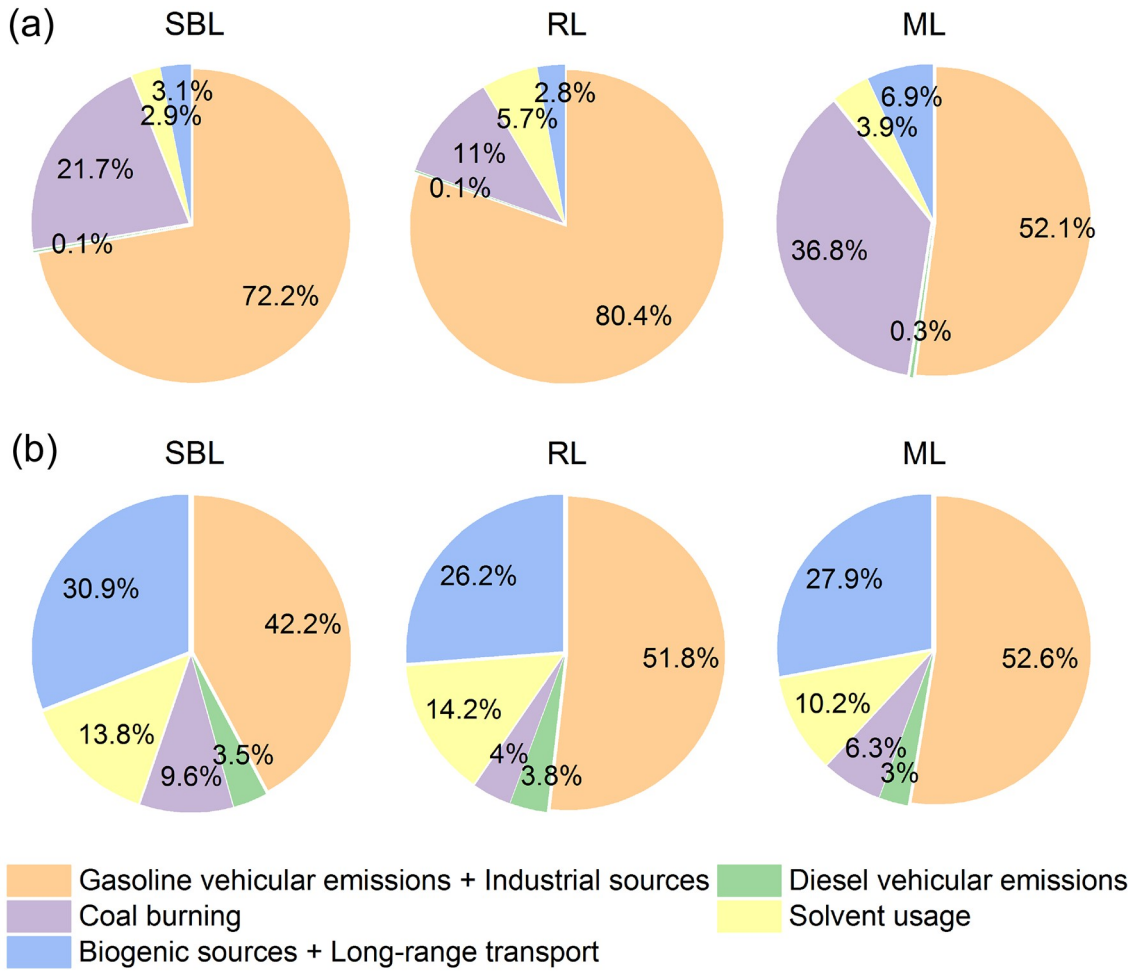

Fig. 8. Source contributions of VOCs in different layers of the PBL above Shijiazhuang in (a) winter and (b) summer derived by PMF.

ively uniform below 600 m and slightly increased from 600 m to 1000 m. Alkanes accounted for the largest proportion at each height, and the proportion gradually increased with height, while the proportions of alkenes, halohydrocarbons, and acetylene gradually decreased. The vertical proportion of aromatics remained almost the same. Isopentane was the species with the highest concentration at each height. The TVOC concentrations and proportions in the SBL and RL at night and in the ML during the day exhibited little difference.

A comparison of the above results with the results of a winter field campaign during 8–16 January 2019 showed that the VOC concentrations and proportions in the vertical direction in winter and summer exhibited significant differences. Except for that of halohydrocarbons, the concentrations of other VOCs in winter were more than twice those in summer, and the ratios between the concentrations in winter and summer were the highest at the surface, decreasing with height. The concentration of halohydrocarbons at high altitudes was slightly higher in summer than in winter. Alkanes accounted for the same proportion in winter and summer. Alkenes, aromatics, and acetylene accounted for higher proportions in winter, while halohydrocarbons accounted for a higher proportion in summer. Vertical VOC sources include gasoline vehicular emissions + industrial sources, coal burning, biogenic sources + long-range transport, solvent usage, and diesel vehicular emissions. The proportions of gasoline vehicular emissions + industrial sources and coal burning were higher in winter. The proportions of biogenic sources + long-range transport, solvent usage, and diesel vehicular emissions were higher in summer. From the surface to 1000 m in winter, the proportions of gasoline vehicular emissions + industrial sources and solvent usage gradually increased. In contrast, the proportion of coal burning gradually decreased. The proportions of diesel vehicular emissions and biogenic sources + long-range transport were relatively uniform. In summer, the proportion of gasoline vehicular emissions + industrial sources gradually increased while the proportions of the other four sources gradually decreased. Measures should be taken, mainly to improve oil quality, to limit the exhaust emissions of motor vehicles to reduce VOC pollution in Shijiazhuang. While gasoline vehicular emissions control is conducive to the reduction of VOC concentrations at the surface, industrial sources control is conducive to the reduction of VOC concentrations at high altitudes.

Acknowledgements. This work was supported by the National Key R&D Program of China (Grant No. 2017YFC021 0000), the National Natural Science Foundation of China (Grant Nos. 41705113 and 41877312), the Young Talent Project of the Center for Excellence in Regional Atmospheric Environment, Chinese Academy of Sciences (Grant No. CERAE20 1802), and a Beijing Major Science and Technology Project (Grant No. Z181100005418014).

REFERENCES

Akimoto, H., 2003: Global air quality and pollution. *Science*, **302**, 1716–1719, https://doi.org/10.1126/science.1092666.

Atkinson, R., and J. Arey, 2003: Atmospheric degradation of volatile organic compounds. *Chemical Reviews*, **103**, 4605–4638, https://doi.org/10.1021/cr0206420.

Bonsang, B., D. Martin, G. Lambert, M. Kanakidou, J. C. Le Roulley, and G. Sennequier, 1991: Vertical distribution of non methane hydrocarbons in the remote marine boundary layer. *J. Geophys. Res.*, **96**, 7313–7324, https://doi.org/10.1029/90JD02539.

Cai, C. J., F. H. Geng, X. X. Tie, Q. Yu, and J. L. An, 2010: Characteristics and source apportionment of VOCs measured in Shanghai, China. *Atmos. Environ.*, **44**, 5005–5014, https://doi.org/10.1016/j.atmosenv.2010.07.059.

Carter, W. P. L., 2010: Development of the SAPRC-07 chemical mechanism. *Atmos. Environ.*, **44**, 5324–5335, https://doi.org/10.1016/j.atmosenv.2010.01.026.

Carter, W. P. L., and G. Heo, 2013: Development of revised SAPRC aromatics mechanisms. *Atmos. Environ.*, **77**, 404–414, https://doi.org/10.1016/j.atmosenv.2013.05.021.

Chen, P., J. N. Quan, Q. Zhang, X. X. Tie, Y. Gao, X. Li, and M. Y. Huang, 2013: Measurements of vertical and horizontal distributions of ozone over Beijing from 2007 to 2010. *Atmos. Environ.*, **74**, 37–44, https://doi.org/10.1016/j.atmosenv.2013.03.026.

Chen, W. T., M. Shao, S. H. Lu, M. Wang, L. M. Zeng, B. Yuan, and Y. Liu, 2014: Understanding primary and secondary sources of ambient carbonyl compounds in Beijing using the PMF model. *Atmospheric Chemistry and Physics*, **14**, 3047–3062, https://doi.org/10.5194/acp-14-3047-2014.

Chen, X. Y., and Coauthors, 2018: Factors dominating 3-dimensional ozone distribution during high tropospheric ozone period. *Environmental Pollution*, **232**, 55–64, https://doi.org/10.1016/j.envpol.2017.09.017.

Gao, W., X. X. Tie, J. M. Xu, R. J. Huang, X. Q. Mao, G. Q. Zhou, and L. Y. Chang, 2017: Long-term trend of O_3 in a mega City (Shanghai), China: Characteristics, causes, and interactions with precursors. *Science of the Total Environment*, **603–604**, 425–433, https://doi.org/10.1016/j.scitotenv.2017.06.099.

Han, T. T., Z. Q. Ma, W. Y. Xu, L. Qiao, Y. R. Li, D. He, and Y. Wang, 2020: Characteristics and source implications of aromatic hydrocarbons at urban and background areas in Beijing, China. *Science of the Total Environment*, **707**, 136083, https://doi.org/10.1016/j.scitotenv.2019.136083.

Islam, M. R., and Coauthors, 2020: Ambient air quality in the Kathmandu Valley, Nepal, during the pre-monsoon: Concentrations and sources of particulate matter and trace gases. *Atmospheric Chemistry and Physics*, **20**, 2927–2951, https://doi.org/10.5194/acp-20-2927-2020.

Koβmann, M., H. Vogel, B. Vogel, R. Vögtlin, U. Corsmeier, F. Fiedler, O. Klemm, and H. Schlager, 1996: The composition and vertical distribution of volatile organic compounds in southwestern Germany, eastern France and northern Switzerland during the TRACT Campaign in September 1992. *Physics and Chemistry of the Earth*, **21**, 429–433, https://doi.org/10.1016/S0079-1946(97)81137-8.

Liu, C. T., Z. B. Ma, Y. J. Mu, J. F. Liu, C. L. Zhang, Y. Y. Zhang, P. F. Liu, and H. X. Zhang, 2017: The levels, variation characteristics, and sources of atmospheric non-methane hydrocarbon compounds during wintertime in Beijing, China. *Atmospheric Chemistry and Physics*, **17**, 10633–10649, https://doi.org/10.5194/acp-17-10633-2017.

Liu, Y., M. Shao, L. L. Fu, S. H. Lu, L. M. Zeng, and D. G. Tang, 2008: Source profiles of volatile organic compounds (VOCs) measured in China: Part I. *Atmos. Environ.*, **42**, 6247–6260, https://doi.org/10.1016/j.atmosenv.2008.01.070.

Liu, Y. F., and Coauthors, 2020: Characterization and sources of volatile organic compounds (VOCs) and their related changes during ozone pollution days in 2016 in Beijing, China. *Environmental Pollution*, **257**, 113599, https://doi.org/10.1016/j.envpol.2019.113599.

Ma, Z. Q., H. H. Xu, W. Meng, X. L. Zhang, J. Xu, Q. Liu, and Y. S. Wang, 2013: Vertical ozone characteristics in urban boundary layer in Beijing. *Environmental Monitoring and Assessment*, **185**, 5449–5460, https://doi.org/10.1007/s10661-012-2958-5.

Ma, Z. Q., J. Xu, W. J. Quan, Z. Y. Zhang, W. L. Lin, and X. B. Xu, 2016: Significant increase of surface ozone at a rural site, north of eastern China. *Atmospheric Chemistry and Physics*, **16**, 3969–3977, https://doi.org/10.5194/acp-16-3969-2016.

Mao, T., Y. S. Wang, J. Jiang, F. K. Wu, and M. X. Wang, 2008: The vertical distributions of VOCs in the atmosphere of Beijing in autumn. *Science of the Total Environment*, **390**, 97–108, https://doi.org/10.1016/j.scitotenv.2007.08.035.

Paatero, P., 1997: Least squares formulation of robust non-negative factor analysis. *Chemometrics and Intelligent Laboratory Systems*, **37**, 23–35, https://doi.org/10.1016/S0169-7439(96)00044-5.

Paatero, P., and U. Tapper, 1994: Positive matrix factorization: A non-negative factor model with optimal utilization of error estimates of data values. *Environmetrics*, **5**, 111–126, https://doi.org/10.1002/env.3170050203.

Richard, A., and Coauthors, 2011: Source apportionment of size and time resolved trace elements and organic aerosols from an urban courtyard site in Switzerland. *Atmospheric Chemistry and Physics*, **11**, 8945–8963, https://doi.org/10.5194/acp-11-8945-2011.

Sangiorgi, G., L. Ferrero, M. G. Perrone, E. Bolzacchini, M. Duane, and B. R. Larsen, 2011: Vertical distribution of hydrocarbons in the low troposphere below and above the mixing height: Tethered balloon measurements in Milan, Italy. *Environmental Pollution*, **159**, 3545–3552, https://doi.org/10.1016/j.envpol.2011.08.012.

Schnitzhofer, R., and Coauthors, 2009: A multimethodological approach to study the spatial distribution of air pollution in an Alpine valley during wintertime. *Atmospheric Chemistry and Physics*, **9**, 3385–3396, https://doi.org/10.5194/acp-9-3385-2009.

Seinfeld, J. H., and S. N. Pandis, 2016: *Atmospheric Chemistry and Physics: From Air Pollution to Climate Change*. 3rd ed., John Wiley & Sons.

Spirig, C., A. Neftel, L. I. Kleinman, and J. Hjorth, 2002: NO_x versus VOC limitation of O_3 production in the Po valley: Local and integrated view based on observations. *J. Geophys. Res.*, **107**, 8191, https://doi.org/10.1029/2001JD000561.

Sun, J., F. K. Wu, B. Hu, G. Q. Tang, J. K. Zhang, and Y. S. Wang, 2016: VOC characteristics, emissions and contributions to SOA formation during hazy episodes. *Atmos. Environ.*, **141**, 560–570, https://doi.org/10.1016/j.atmosenv.2016.06.060.

Sun, J., Y. S. Wang, F. K. Wu, G. Q. Tang, L. L. Wang, Y. H. Wang, and Y. Yang, 2018: Vertical characteristics of VOCs in the lower troposphere over the North China Plain during pollution periods. *Environmental Pollution*, **236**, 907–915, https://doi.org/10.1016/j.envpol.2017.10.051.

Tang, G., X. Li, Y. Wang, J. Xin, and X. Ren, 2009: Surface ozone trend details and interpretations in Beijing, 2001-2006. *Atmospheric Chemistry and Physics*, **9**, 8813–8823, https://doi.org/10.5194/acp-9-8813-2009.

Tang, G., Y. Wang, X. Li, D. Ji, S. Hsu, and X. Gao, 2012: Spatial-temporal variations in surface ozone in Northern China as observed during 2009–2010 and possible implications for future air quality control strategies. *Atmospheric Chemistry and Physics*, **12**, 2757–2776, https://doi.org/10.5194/acp-12-2757-2012.

Tang, G., X. Zhu, B. Hu, J. Xin, L. Wang, C. Münkel, G. Mao, and Y. Wang, 2015: Impact of emission controls on air quality in Beijing during APEC 2014: Lidar ceilometer observations. *Atmospheric Chemistry and Physics*, **15**, 12667–12680, https://doi.org/10.5194/acp-15-12667-2015.

Tang, G. Q., N. Chao, Y. S. Wang, and J. S. Chen, 2016: Vehicular emissions in China in 2006 and 2010. *Journal of Environmental Sciences*, **48**, 179–192, https://doi.org/10.1016/j.jes.2016.01.031.

Tang, G. Q., and Coauthors, 2017: Modelling study of boundary-layer ozone over northern China - Part I: Ozone budget in summer. *Atmospheric Research*, **187**, 128–137, https://doi.org/10.1016/j.atmosres.2016.10.017.

Tang, G. Q., and Coauthors, 2021: Bypassing the NOx titration trap in ozone pollution control in Beijing. *Atmospheric Research*, **249**, 105333, https://doi.org/10.1016/j.atmosres.2020.105333.

Wöhrnschimmel, H., C. Márquez, V. Mugica, W. A. Stahel, J. Staehelin, B. Cárdenas, and S. Blanco, 2006: Vertical profiles and receptor modeling of volatile organic compounds over Southeastern Mexico City. *Atmos. Environ.*, **40**, 5125–5136, https://doi.org/10.1016/j.atmosenv.2006.03.008.

Wu, S., and Coauthors, 2020: Vertically decreased VOC concentration and reactivity in the planetary boundary layer in winter over the North China Plain. *Atmospheric Research*, **240**, 104930, https://doi.org/10.1016/j.atmosres.2020.104930.

Yang, X. Y., and Coauthors, 2020: Summertime ozone pollution in Sichuan Basin, China: Meteorological conditions, sources and process analysis. *Atmos. Environ.*, **226**, 117392, https://doi.org/10.1016/j.atmosenv.2020.117392.

Yang, Y., and Coauthors, 2019: Ambient volatile organic compounds in a suburban site between Beijing and Tianjin: Concentration levels, source apportionment and health risk assessment. *Science of the Total Environment*, **695**, 133889, https://doi.org/10.1016/j.scitotenv.2019.133889.

Yue, X., and Coauthors, 2017: Ozone and haze pollution weakens net primary productivity in China. *Atmospheric Chemistry and Physics*, **17**, 6073–6089, https://doi.org/10.5194/acp-17-6073-2017.

Yurdakul, S., M. Civan, Ö. Kuntasal, G. Doğan, H. Pekey, and G. Tuncel, 2018: Temporal variations of VOC concentrations in Bursa atmosphere. *Atmospheric Pollution Research*, **9**, 189–206, https://doi.org/10.1016/j.apr.2017.09.004.

Zhang, C. X., and Coauthors, 2019: Satellite UV-Vis spectroscopy: Implications for air quality trends and their driving forces in China during 2005–2017. *Light: Science & Applications*, **8**, 100, https://doi.org/10.1038/s41377-019-0210-6.

Zhang, K., G. L. Xiu, L. Zhou, Q. G. Bian, Y. S. Duan, D. N. Fei,

D. F. Wang, and Q. Y. Fu, 2018: Vertical distribution of volatile organic compounds within the lower troposphere in late spring of Shanghai. *Atmos. Environ.*, **186**, 150–157, https://doi.org/10.1016/j.atmosenv.2018.03.044.

Zhang, Q., and Coauthors, 2014: Variations of ground-level O_3 and its precursors in Beijing in summertime between 2005 and 2011. *Atmospheric Chemistry and Physics*, **14**, 6089–6101, https://doi.org/10.5194/acp-14-6089-2014.

Zhao, W., and Coauthors, 2019: Evolution of boundary layer ozone in Shijiazhuang, a suburban site on the North China plain. *Journal of Environmental Sciences*, **83**, 152–160, https://doi.org/10.1016/j.jes.2019.02.016.

Zheng, X., G. Ding, Y. U. Haiqing, Y. Liu, and X. U. Xiangde, 2005: Vertical distribution of ozone in the planetary boundary layer at the Ming Tombs, Beijing. *Science in China Series D Earth Sciences*, **48**, 55–63.